

# Chapter 6—Outline

## Interference by Division of Amplitude

<b>Chapter 6: Interference by Division of Amplitude</b> . . . . .	165
<b>6.1</b> Introduction . . . . .	165
<b>6.2</b> Introduction to the Michelson Interferometer . . . . .	165
<b>6.3</b> Michelson Interferometer: Circular Fringes . . . . .	166
<b>6.3.1</b> Derivations . . . . .	166
<b>6.3.2</b> Circular fringes for a monochromatic source . . . . .	168
Bright fringes . . . . .	168
Bright fringes when $r = 0$ . . . . .	168
Bright fringes as a function of $r$ . . . . .	168
Graphs of the circular fringes . . . . .	169
<b>6.3.3</b> Circular fringes for a doublet . . . . .	170
<b>6.4</b> Visibility of Fringes . . . . .	171
<b>6.4.1</b> Introduction . . . . .	171
<b>6.4.2</b> The spectral intensity $I(\sigma)$ . . . . .	172
<b>6.4.3</b> The visibility $V$ . . . . .	172
<b>6.4.4</b> Gaussian $I(\sigma')$ . . . . .	175
<b>6.4.5</b> Lorentzian $I(\sigma')$ . . . . .	176
<b>6.4.6</b> Sodium-like D lines $I(\sigma')$ . . . . .	177
<b>Problems</b> . . . . .	178
<b>Answers to Problems</b> . . . . .	180

**Page intentionally left blank.**

# Chapter 6

## Interference by Division of Amplitude

### 6.1 Introduction

Many of the properties of light are described by modeling light in terms of traveling harmonic waves, or a superposition (or addition) of several or many such waves. If the harmonic waves have a constant wavelength  $\lambda$ , we say the light is monochromatic (one color). If the crests and troughs of the waves travel “in step” and “side-by-side,” we say the light is coherent. The diagram in Figure 6.1, which is similar to the earlier diagrams of Figures 5.24 and 5.25, is an example of waves that are both monochromatic and coherent. However, light from most sources is neither monochromatic nor coherent; the exception is laser light.

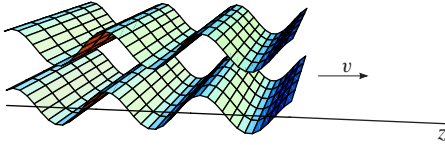


**Figure 6.1** Monochromatic, coherent waves.

One interesting property of traveling harmonic waves is that they can interfere with themselves or other waves. That is, if a crest of a wave travels through a region at the same time the crest of another wave travels through the region, the two crests add to give a bigger wave; or in terms of light, brighter light—this behavior is called constructive interference. Conversely, if a crest of a wave is superimposed on a trough of another wave, the crest and trough add algebraically to give a smaller wave, or if the trough is as deep as the crest is high, nothing at all; for light, dimmer light or darkness—this action is called destructive interference.

Interference phenomena are divided into two classes: division of wavefront and division of amplitude. In the familiar double-slit interference, the interference is division of wavefront because wavefronts falling on the double slit become pairs of wavefronts on the other side of the slits. Division of amplitude occurs in the Michelson interferometer, the subject of this chapter.

### 6.2 Introduction to the Michelson Interferometer

An idealized Michelson interferometer is shown in the diagram of Figure 6.2. An on-axis, monochromatic (but not necessarily coherent) light wave of amplitude  $E_0$  from a source  $S$  falls at  $45^\circ$  onto a beam splitter (a plate of glass the back side of which is lightly silvered) which halves the incident wave into two waves: one wave is transmitted, has

amplitude  $E_0/2$ , and is reflected by the fixed mirror  $M_1$  back to the beam splitter where another half (amplitude  $E_0/4$ ) is reflected to the eye or other detector; the other wave is reflected at the beam splitter, has amplitude  $E_0/2$ , and is reflected by the movable mirror  $M_2$  back to the beam splitter where half is transmitted (amplitude  $E_0/4$ ) to the eye. In actual practice the  $E_0/2$  and  $E_0/4$  amplitudes are not quite these values because of additional (usually small) reflections and absorptions that we are omitting in the idealized Michelson interferometer.

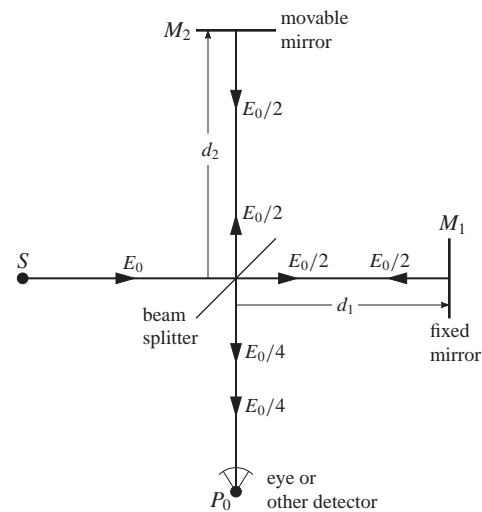


**Figure 6.2** The idealized Michelson interferometer.

If the interferometer is in air, then the index of refraction  $n$  of the air is close enough to one that we can set  $n = 1$ . By inspection of Figure 6.2, we determine the optical path difference  $\Delta$  using Equation 5.98 as a guide:

$$\begin{aligned}\Delta &= \ell_2 - \ell_1 = n(2d_2) - n(2d_1) \\ &= 2(d_2 - d_1) = 2d\end{aligned}\quad (6.1)$$

where

$$d = d_2 - d_1 \quad (6.2)$$

The corresponding phase difference  $\delta$  is found from Equation 5.97, and after we substitute Equation 6.1, we get

$$\delta = \frac{2\pi}{\lambda} \Delta = \frac{4\pi d}{\lambda} \quad (6.3)$$

We now give a summary of the wave behavior. Many monochromatic waves are emitted by the source  $S$ . We concentrate our attention on one of these waves. It travels to the

beam splitter where it is divided in half, one of these halves (call it  $E_1$ ) travels to mirror  $M_1$ , is reflected back to the beam splitter where half is reflected to the point  $P_0$ . The other half (call it  $E_2$ ) is reflected by the beam splitter to mirror  $M_2$ , there it is reflected back to the beam splitter where half is transmitted to the point  $P_0$ . So at the point  $P_0$ , we have two waves,  $E_1(P_0)$  and  $E_2(P_0)$ , each of amplitude  $E_0/4$ , differing in phase by  $\delta$ , that interfere (or add or superimpose) to give a new wave  $E(P_0)$ . In equation form, we have (see discussion for Figures 5.28 and 5.29, and Equations 5.105 and 5.106)

$$\begin{aligned} E(P_0) &= E_1(P_0) + E_2(P_0) \\ &= \frac{E_0}{4} \cos(\omega t) + \frac{E_0}{4} \cos(\omega t - \delta) \end{aligned} \quad (6.4)$$

The corresponding complex form is

$$\mathbf{E}(P_0) = \frac{E_0}{4} e^{i(\omega t)} + \frac{E_0}{4} e^{i(\omega t - \delta)} \quad (6.5)$$

To calculate the intensity at the point  $P_0$ , we use Equation 5.85 and the complex expression of  $\mathbf{E}$  in Equation 6.5:

$$\begin{aligned} I(P_0) &= C \mathbf{E} \mathbf{E}^* \\ &= C \left[ \frac{E_0}{4} e^{i(\omega t)} + \frac{E_0}{4} e^{i(\omega t - \delta)} \right] \\ &\quad \left[ \frac{E_0}{4} e^{-i(\omega t)} + \frac{E_0}{4} e^{-i(\omega t - \delta)} \right] \\ &= C \left( \frac{E_0^2}{16} + \frac{E_0^2}{16} e^{-i\delta} + \frac{E_0^2}{16} e^{i\delta} + \frac{E_0^2}{16} \right) \\ &= \frac{C E_0^2}{16} (2 + e^{-i\delta} + e^{i\delta}) \\ &= \frac{C E_0^2}{16} (2 + \cos \delta - i \sin \delta + \cos \delta + i \sin \delta) \\ &= \frac{C E_0^2}{8} (1 + \cos \delta) \\ &= \frac{I_0}{8} (1 + \cos \delta) \end{aligned} \quad (6.6)$$

where we have used Euler's identity (see Equation 5.11) to convert from the polar to rectangular form, and where

$$I_0 = C E_0^2 \quad (6.7)$$

is the intensity of the incident wave that leaves the point  $S$  in Figure 6.2. Applying the trig identity

$$1 + \cos A = 2 \cos^2 \frac{A}{2} \quad (6.8)$$

where  $A$  is any angle, in Equation 6.6, we obtain

$$I = \frac{I_0}{4} \cos^2 \frac{\delta}{2} = I_m \cos^2 \frac{\delta}{2} \quad (6.9)$$

where

$$I_m = \frac{I_0}{4} \quad (6.10)$$

is the maximum intensity. As we discussed in Section 5.3.4, the units of  $I$  are  $\text{W}/\text{m}^2$ .

According to Equation 6.3, we have  $\delta = 4\pi d/\lambda$ , which means that  $\delta$  varies as the mirror  $M_2$  is moved. Looking at Equation 6.9, we see that a changing  $\delta$  implies that  $I$  will change from a maximum of  $I_m$  to a minimum of zero. This behavior means that as we look straight into the interferometer, as depicted in Figures 6.2 and 6.3, we would see the light intensity vary from bright to dark as mirror  $M_2$  moves. Next, we want to investigate this behavior more generally.

## 6.3 Michelson Interferometer: Circular Fringes

### 6.3.1 Derivations

We first simplify the idealized Michelson interferometer that we diagrammed in Figure 6.2 by drawing the image  $M'_1$  of the mirror  $M_1$  that the eye sees when it looks into the beam splitter, as shown in Figure 6.3. By inspection, we observe that Equations 6.1, 6.2, and 6.3 are all still true; and we have an easier diagram to use.

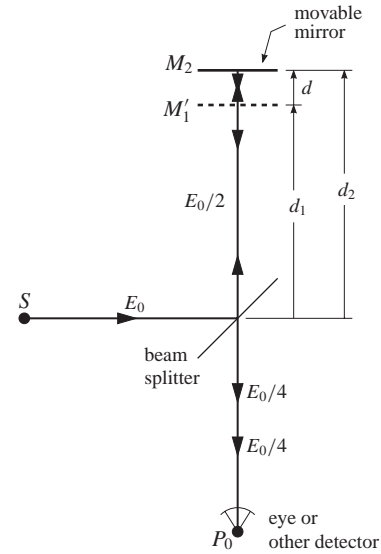


**Figure 6.3** The idealized Michelson interferometer simplified by reflecting the fixed mirror in the beam splitter.

However, the diagram in Figure 6.3 still shows only the on-axis waves that travel through the interferometer to produce an intensity at the point  $P_0$  that varies between bright and dark spots. To make the diagram more general and obtain circular fringes, as well as the spots at  $P_0$ , we must draw the paths (or rays) followed by off-axis waves. We draw this diagram in Figure 6.4. To increase the brightness of the fringes, we use an extended source  $S$  instead of the point source we used in the previous diagrams; an extended source is usually made by allowing the light from a physical source to pass through a thin plate of frosted glass. We show two rays (that the waves follow) from the extended source in this diagram; these rays

are reflected by the beam splitter up to the mirrors  $M'_1$  and  $M_2$ , where they are reflected again to pass down to the detector, which we imagine to be an eye (obviously, the eyelens is not drawn to scale). In the diagram of Figure 6.4, we imagine that the eye is focused at  $-\infty$  so that only parallel rays from  $S$  are focused at the point  $P$  on the focal plane of the eye.

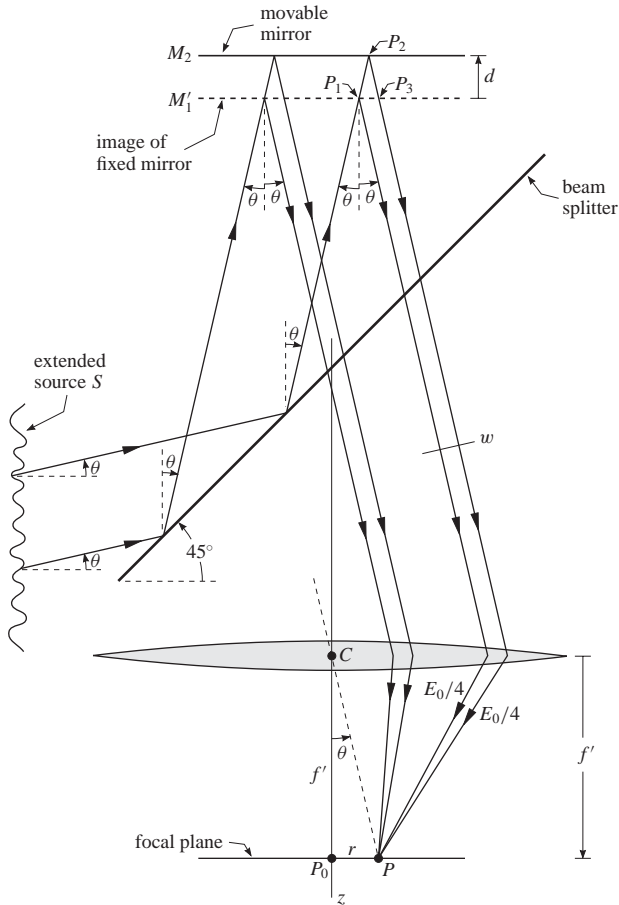


**Figure 6.4** An expanded view of the idealized Michelson interferometer.

Actually, many more rays than the two shown leaving the source  $S$  arrive at  $P$ ; in fact, all rays parallel to the two depicted reach  $P$ , which increases the intensity—important because the intensity is usually not large. We know that each pair of parallel rays falling on the lens is focused on the point  $P$  by drawing an imagined ray (the dashed line) through the lens center  $C$  parallel to the set—such a ray passes through the lens undeviated in direction as we learned in chapter 1.

The line  $w$  drawn perpendicular to a pair of rays in Figure 6.4 represents a wavefront. The waves traveling along this pair of rays when compared on this wavefront have a phase difference  $\delta$ , which is maintained through the lens to the point  $P$  where the waves interfere. The phase difference  $\delta$  remains the same from  $w$  to  $P$  because the optical path measured from  $w$  to  $P$  is constant through the third order in  $R$ , where  $R$  is the distance from  $C$  to a ray in the middle of the lens (as we discussed in Section 3.5). In fact,  $\delta$  is the same

for any wavefront parallel to  $w$  on the pair of rays. The same argument holds for all pairs of rays reaching the point  $P$ .

We now want to calculate the phase difference  $\delta$ ; in fact, the main reason for drawing  $M'_1$  as the image of the fixed mirror in Figure 6.4 is to help us calculate  $\delta$ . To obtain  $\delta$ , we need to determine the optical path difference  $\Delta$ . By inspecting Figure 6.4, we see that  $\Delta$  becomes nonzero when the wave arrives at point  $P_1$  where it divides and follows two different paths. We enlarge the diagram in this vicinity in Figure 6.5, and add some labeling. First of all, we observe

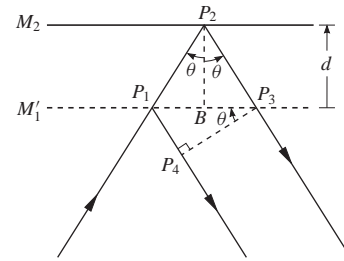


**Figure 6.5**

that the line  $P_3P_4$  in Figure 6.5 is perpendicular to the pair of parallel rays; therefore, it represents a wavefront parallel to the wavefront  $w$  in Figure 6.4, and so the optical path from  $P_1$  to  $P$  is the same as from  $P_4$  to  $P$  by the argument given in the previous paragraph. The optical path difference  $\Delta$  arises from the difference in the optical paths  $\overline{P_1P_2P_3}$  and  $\overline{P_1P_4}$ . By inspection of Figure 6.5, we see that

$$\overline{P_1P_2} = \overline{P_2P_3} = \frac{d}{\cos \theta}$$

$$\overline{P_1B} = \overline{BP_3} = d \tan \theta$$

$$\overline{P_1P_3} = 2d \tan \theta$$

$$\overline{P_1P_4} = \overline{P_1P_3} \sin \theta = (2d \tan \theta) \sin \theta$$

Remembering that the waves are traveling in air so  $n = 1$ , we use the above expressions and several trig identities to calculate the optical path difference:

$$\begin{aligned} \Delta &= n \overline{P_1P_2P_3} - n \overline{P_1P_4} = n \overline{P_1P_2} + n \overline{P_2P_3} - n \overline{P_1P_4} \\ &= \frac{d}{\cos \theta} + \frac{d}{\cos \theta} - (2d \tan \theta) \sin \theta \\ &= 2d \left( \frac{1}{\cos \theta} - \frac{\sin \theta}{\cos \theta} \sin \theta \right) \\ &= 2d \frac{1 - \sin^2 \theta}{\cos \theta} = 2d \frac{\cos^2 \theta}{\cos \theta} = 2d \cos \theta \end{aligned} \quad (6.11)$$

By Equation 5.97, the phase difference is then

$$\delta = \frac{2\pi}{\lambda} \Delta = \frac{4\pi d}{\lambda} \cos \theta \quad (6.12)$$

which reduces to Equation 6.3 when  $\theta = 0$ , as it should.

Now that we know the phase difference  $\delta$ , we can add the two waves of amplitude  $E_0/4$  at the point  $P$  (see Figure 6.4). In complex form we have

$$\begin{aligned} \mathbf{E}(P) &= \mathbf{E}_1(P) + \mathbf{E}_2(P) \\ &= \frac{E_0}{4} e^{i(\omega t)} + \frac{E_0}{4} e^{i(\omega t - \delta)} \end{aligned} \quad (6.13)$$

which is just like Equation 6.5 except we add the waves at  $P$  instead of  $P_0$ , and  $\delta$  is given by Equation 6.12. Because Equation 6.13 is symbolically the same as Equation 6.5, we can determine the intensity  $I$  at  $P$  just like we did to get Equations 6.6 and 6.9:

$$I(P) = \frac{I_0}{8} (1 + \cos \delta) = I_m \cos^2 \frac{\delta}{2} \quad (6.14)$$

where (see Equations 6.7 and 6.10)

$$I_0 = C E_0^2 \quad \text{and} \quad I_m = \frac{I_0}{4} \quad (6.15)$$

and  $\delta$  is given by Equation 6.12. By inspection of Figure 6.4, we obtain the radius  $r$  of the circular fringes:

$$r = f' \tan \theta \quad (6.16)$$

That the fringes in the focal plane of Figure 6.4 are circles of radius  $r$  can be inferred from the symmetry of the mirrors and lens about the  $z$  axis. Using Figure 6.4 as a guide, we draw the right triangle for  $f'$  and  $r$  in Figure 6.6; then we work out an expression for the hypotenuse and see that

$$\cos \theta = \frac{f'}{\sqrt{f'^2 + r^2}} = \frac{1}{\sqrt{1 + (r/f')^2}} \quad (6.17)$$

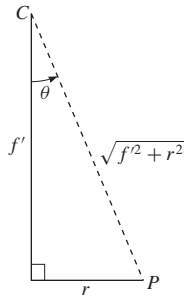


Figure 6.6

In actual practice, when the fringe pattern is viewed as depicted in Figure 6.4, what we see is an intensity that varies with the radius  $r$ . To obtain an  $I$  versus  $r$  equation, we start with Equation 6.14 and substitute Equations 6.12 and 6.17; we get

$$I(P) = I_m \cos^2 \frac{\delta}{2} = I_m \cos^2 \left( \frac{2\pi d/\lambda}{\sqrt{1 + (r/f')^2}} \right) \quad (6.18)$$

We now want to study the properties of this equation.

### 6.3.2 Circular fringes for a monochromatic source

**Bright fringes.** Looking at Equation 6.18, we see that bright fringes will occur with an intensity of  $I_m$  when the argument of  $\cos^2$  is a multiple of  $\pi$ ; that is,

$$\frac{2\pi d/\lambda}{\sqrt{1 + (r/f')^2}} = m\pi, \quad m = \dots - 1, 0, 1, \dots \quad (6.19)$$

We have included the negative integers for  $m$  because  $d$  can be negative when mirror  $M_2$  is below  $M_1'$  (see Figure 6.4); the other quantities are positive. Canceling the  $\pi$ s in Equation 6.19, we get

$$\frac{2d/\lambda}{\sqrt{1 + (r/f')^2}} = m, \quad m = \dots - 1, 0, 1, \dots \quad (6.20)$$

A somewhat similar equation is obtained for dark fringes; that is, when the intensity  $I = 0$ .

**Bright fringes when  $r = 0$ .** At the center of the circular fringes  $r = 0$ , and Equation 6.20 becomes

$$\frac{2d}{\lambda} = m, \quad m = \dots - 1, 0, 1, \dots \quad (6.21)$$

If we take differentials of this equation holding  $\lambda$  constant, and then solve for  $\lambda$ , we get

$$\lambda = \frac{2 \Delta d}{\Delta m} = \frac{2 \Delta d}{N} \quad (6.22)$$

where  $\Delta d$  is a change in the separation  $d$  that causes  $\Delta m = N$  fringes (or bright spots) to appear at the center of the pattern. Usually, a micrometer screw is used to change  $d$  by moving  $M_2$ , and the number of fringes  $N$  is counted visually or by a digital counter. Equations 6.21 and 6.22 continue to hold even for  $r \neq 0$  as long as  $r/f' \ll 1$ .

**Bright fringes as a function of  $r$ .** We assume all the quantities on the left side in Equation 6.20 to have fixed values except  $r$ . For convenience, suppose that  $r$  can only run through values from 0 to  $f'$  so that  $0 \leq r/f' \leq 1$ . Now as  $r$  runs through these values, we imagine that we evaluate the left side of Equation 6.20: whenever the evaluation is an integer, then we have found a radius  $r$  of a bright fringe.

To see the range of the  $m$  values when  $0 \leq r/f' \leq 1$ , we first solve Equation 6.20 for  $r/f'$ :

$$\frac{r}{f'} = \sqrt{\left( \frac{2d}{m\lambda} \right)^2 - 1} \quad (6.23)$$

and then manipulate with inequalities:

$$0 \leq \sqrt{\left( \frac{2d}{m\lambda} \right)^2 - 1} \leq 1$$

$$0 \leq \left( \frac{2d}{m\lambda} \right)^2 - 1 \leq 1$$

$$1 \leq \left( \frac{2d}{m\lambda} \right)^2 \leq 2$$

and when  $d \geq 0$ , we have

$$\begin{aligned}
 1 &\leq \frac{2d}{m\lambda} \leq \sqrt{2} \\
 1 &\geq \frac{m\lambda}{2d} \geq \frac{1}{\sqrt{2}} \\
 2\frac{d}{\lambda} &\geq m \geq \frac{2}{\sqrt{2}}\frac{d}{\lambda} \\
 \frac{2}{\sqrt{2}}\frac{d}{\lambda} &\leq m \leq 2\frac{d}{\lambda}, \quad d \geq 0 \quad (6.24a)
 \end{aligned}$$

If  $d < 0$ , then  $m$  runs through negative values as given by

$$2\frac{d}{\lambda} \leq m \leq \frac{2}{\sqrt{2}}\frac{d}{\lambda}, \quad d < 0 \quad (6.24b)$$

For example, suppose  $d/\lambda = 5.25$ ; that is,  $d$  is positive and 5.25 times larger than  $\lambda$ . Then Equation 6.24a says that  $7.4 \leq m \leq 10.5$ , which means that  $m$  may be any of the integers 8, 9, 10. If we substitute these values into Equation 6.23, and in addition make the  $m$  values one less and one greater than the ones in the range just given (to see what happens), we get the results listed in the table of Figure 6.7. We observe that when  $m = 7$ , then  $r/f' > 1$ , and when  $m = 11$ , then  $r/f'$  is imaginary: these results are consistent with what we would expect. We note the inverse relationship between  $m$  and  $r/f'$ .

$\frac{d}{\lambda} = 5.25$	$m$	$r/f'$
	7	1.118
	8	0.850
	9	0.601
	10	0.320
	11	$i0.298$

Figure 6.7

**Graphs of the circular fringes.** We look at Figure 6.4 to remind us that the fringe pattern is produced on the focal plane. The fringe pattern is circular and in two dimensions; we want to draw a representation of that pattern by taking a one-dimensional slice, as is actually indicated in Figure 6.4. To graph this slice, we take Equation 6.18 and rewrite it as

$$\frac{I}{I_m} = \cos^2 \left( \frac{2\pi d/\lambda}{\sqrt{1 + (r/f')^2}} \right) \quad (6.25)$$

Inspection of this equation suggests that we should choose values for  $d/\lambda$  and then graph  $I/I_m$  versus  $r/f'$ . Since we have been choosing 5.25 as a value for  $d/\lambda$  in our work so far, we make this choice for the first graph in Figure 6.8, where we continue to let  $r/f'$  range from 0 to 1. Then we draw a second graph for  $d/\lambda = 5.1$  and a third for  $d/\lambda = 5$ . The  $m$  values are written above the bright fringes in each of the graphs. We observe that the  $m$  values are 10, 9, 8, as we

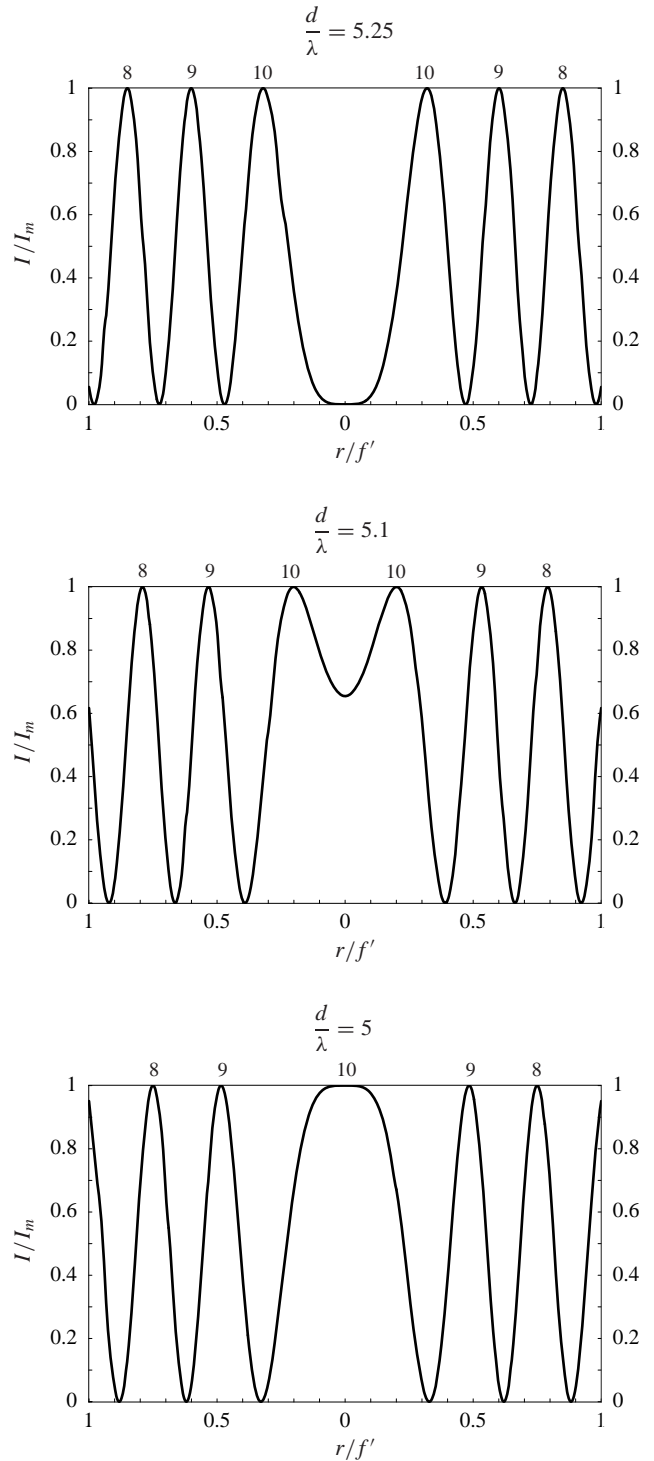


Figure 6.8

would expect from the table in Figure 6.7; in fact, for the graph that corresponds to  $d/\lambda = 5.25$ , we see that the  $r/f'$  values in the graph match those in the Figure 6.7 table, as they should. We also note how the  $m$  values are larger near the center of the graph ( $r/f' = 0$ ) and become smaller away from the center—consistent with the inverse relationship between  $m$  and  $r/f'$  in the table of Figure 6.7.

We chose a range for  $r/f'$  from 0 to 1, and rather small values for  $d/\lambda$ , so that we would have something rather simple with which to work. Actually, in practice  $r/f'$  has a much smaller range, and the fringes for small  $d/\lambda$  become messy and spread out because the mirrors are not perfectly flat.

### 6.3.3 Circular fringes for a doublet

Many sources of light emit waves that are doublets; that is, the waves are composed of two wavelengths that are nearly equal. For example, sodium light has a doublet in the visible region of

$$\left. \begin{aligned} \lambda_1 &= 588.995 \text{ nm} \\ \lambda_2 &= 589.592 \text{ nm} \end{aligned} \right\} \quad (6.26)$$

which gives

$$\Delta\lambda = \lambda_2 - \lambda_1 = 0.597 \text{ nm} \quad (6.27)$$

With the Michelson interferometer, we can measure all three of these values:  $\lambda_1$ ,  $\lambda_2$ , and  $\Delta\lambda$ .

The measurement of  $\Delta\lambda$  is based on the fact that when  $|d|$  is small the fringes are sharp and are clearly visible, but as  $|d|$  is made larger, the fringes fade away and essentially disappear—we use absolute values for  $d$ , because  $|d|$  can be positive or negative depending on the movable mirror being above or below the fixed mirror (see Figure 6.4). As  $|d|$  is made yet larger, the fringes again appear clearly and then fade away a second time. This alternate appearing and disappearing can be repeated many times as  $|d|$  is increased to larger and larger values.

The fringes from a doublet are composed of the sum  $I_{\text{tot}}$  of two intensities,  $I_1$  and  $I_2$ , where  $I_1$  is the intensity of the pattern produced by the waves of wavelength  $\lambda_1$ , and  $I_2$  from the waves of wavelength  $\lambda_2$ . Looking at Equation 6.14 for a monochromatic source, we infer that for two sources

$$\begin{aligned} I_{\text{tot}} &= I_1 + I_2 \\ &= \frac{I_{01}}{8}(1 + \cos \delta_1) + \frac{I_{02}}{8}(1 + \cos \delta_2) \end{aligned} \quad (6.28a)$$

$$= \frac{I_m}{2} \cos^2 \frac{\delta_1}{2} + \frac{I_m}{2} \cos^2 \frac{\delta_2}{2} \quad (6.28b)$$

and from Equation 6.12

$$\delta_1 = \frac{2\pi \Delta}{\lambda_1} = \frac{4\pi d}{\lambda_1} \cos \theta \quad (6.29a)$$

$$\delta_2 = \frac{2\pi \Delta}{\lambda_2} = \frac{4\pi d}{\lambda_2} \cos \theta \quad (6.29b)$$

We write  $I_m/2$  in Equation 6.28b because what we really view is  $I_{\text{tot}}$ ; thus it is more realistic to express the components that compose  $I_{\text{tot}}$  in terms of the maximum  $I_m$  of  $I_{\text{tot}}$ . We assume the same maximum intensities  $I_m/2$  for simplicity.

Just as in Figure 6.8, we want to graph the intensity ratios versus  $r/f'$ . We substitute Equations 6.29 into the  $I_1$  and  $I_2$  expressions of Equation 6.28b, then divide through by  $I_m$  to get

$$\frac{I_1}{I_m} = \frac{1}{2} \cos^2 \left( \frac{2\pi d/\lambda_1}{\sqrt{1 + (r/f')^2}} \right) \quad (6.30a)$$

$$\frac{I_2}{I_m} = \frac{1}{2} \cos^2 \left( \frac{2\pi d/\lambda_2}{\sqrt{1 + (r/f')^2}} \right) \quad (6.30b)$$

and

$$\frac{I_{\text{tot}}}{I_m} = \frac{I_1}{I_m} + \frac{I_2}{I_m} \quad (6.30c)$$

We graph the intensity ratios of Equations 6.30 in the three graphs of Figure 6.9 using the sodium wavelengths in Equation 6.26 for  $\lambda_1$  and  $\lambda_2$ . As we indicate in the diagrams,  $I_{\text{tot}}/I_m$  is the solid curve,  $I_1/I_m$  is the dotted curve, and  $I_2/I_m$  is the dashed curve; the  $m$  values for the peaks of  $I_1/I_m$  and  $I_2/I_m$  are also indicated (the  $m_1$  values go with  $I_1/I_m$ , the  $m_2$  with  $I_2/I_m$ ). We imagine these diagrams are snapshots of the curves for three different  $d$  values (see Figure 6.4) as we slowly turn the micrometer screw to increase  $d$ . We allow  $r/f'$  to vary only to 0.1 to get reasonable-looking graphs. The curves move outward from the center as  $d$  increases.

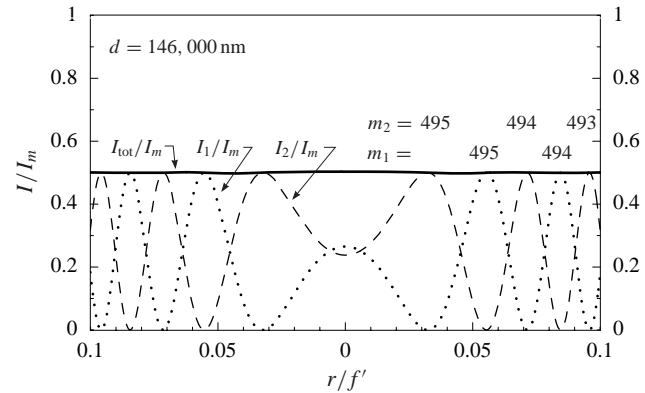


**Figure 6.9(a)** The  $I_1/I_m$  and  $I_2/I_m$  curves are about  $180^\circ$  out of phase to give an almost constant  $I_{\text{tot}}/I_m$ .

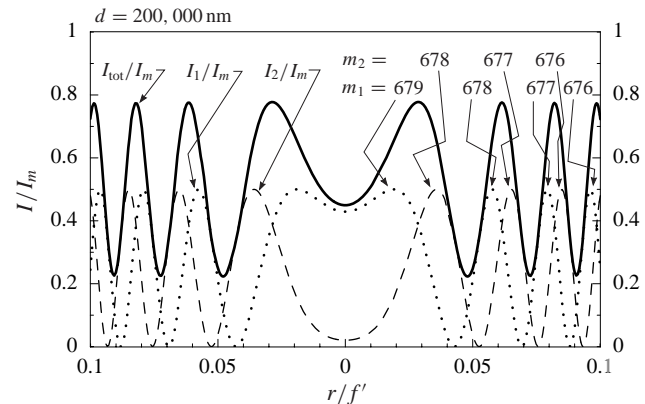


**Figure 6.9(b)** The  $I_1/I_m$ ,  $I_2/I_m$  curves move toward an in-phase position to give a noticeable variation to  $I_{\text{tot}}/I_m$ .



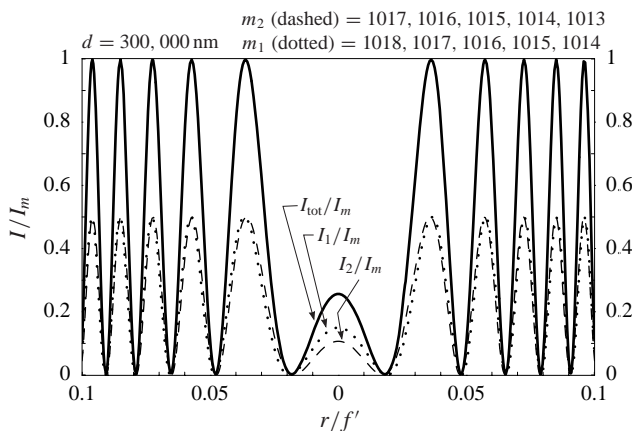


**Figure 6.9(c)** The  $I_1/I_m$ ,  $I_2/I_m$  curves are almost exactly in phase to make a maximum variation of  $I_{tot}/I_m$ .

In the above diagram of Figure 6.9(c), the curves for  $I_1/I_m$  and  $I_2/I_m$  are almost in phase when  $d = 300,000$  nm; they add to give the sum  $I_{tot}/I_m$ , which varies from a minimum and maximum of close to zero and one, respectively. Also, note that the order number  $m_1$  for the smaller wavelength  $\lambda_1$  is one greater than  $m_2$  for overlapping fringes.

The variation in  $I_{tot}/I_m$  from an almost constant where the fringes disappear (Figure 6.9(a)) to where they are clearly seen, as indicated in Figure 6.9(c), repeats several times as  $d$  is increased—this behavior is described as the visibility of the fringes.

## 6.4 Visibility of Fringes

### 6.4.1 Introduction

So far we have assumed that the source  $S$  emitted perfectly monochromatic waves of wavelength  $\lambda$ , or emitted a pair of waves with wavelengths  $\lambda_1$  and  $\lambda_2$  that were approximately the same (a doublet).

But when real, monochromatic sources are used, even laser sources, it is found that as  $|d|$  is increased, the fringes seen in the Michelson interferometer are at first sharply visible and then fuzz out and essentially disappear in a manner similar to the doublet we analyzed before (except they don't reappear). For spectral line sources (such as mercury vapor, or gases of hydrogen and helium), the disappearance of the fringes occurs when  $|d|$  is of the order of millimeters, whereas for lasers it can be kilometers. Therefore, real sources are only approximately monochromatic, and investigation shows that we must think of a real, monochromatic source as emitting many wavelengths centered about a central wavelength that we normally use as the monochromatic value—or, as will be more convenient in this section, instead of using the wavelength  $\lambda$  to characterize the waves, we shall use the wave number  $\sigma = 1/\lambda$  (for review, see the table in Figure 5.23).

An alternative explanation of the fringe disappearance, but completely equivalent, is to say that the harmonic waves making up the light have only a finite length, called a wave train. If  $|d|$  is small, then the wave train from one arm will overlap most of the train from the other arm, as shown in Figure 6.10(a). But if  $|d|$  is large, then the wave trains do not overlap anymore, as shown in Figure 6.10(b), and the visibility of the fringes disappears.

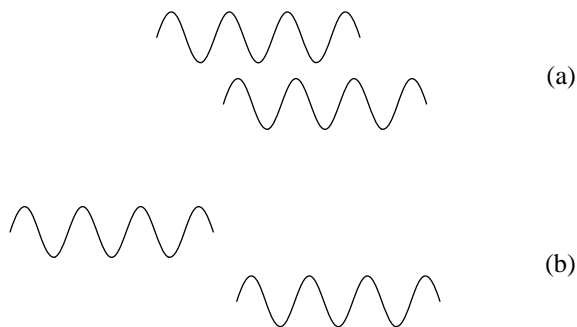


**Figure 6.10**

In our work with the Michelson interferometer, it is more convenient to consider a real monochromatic source as one that emits many wavelengths, rather than wave trains of finite length. As we mentioned before, we want to use wave numbers  $\sigma$  (it makes the math somewhat simpler) to describe the waves. Thus, for a monochromatic wave, such as those we discussed in previous sections, we represent the intensity  $I(\sigma)$  as a function of  $\sigma$  in the diagram of Figure 6.11(a), where  $\sigma_0$  is the monochromatic wave number and the intensity is nonzero only at this value. This picture corresponds to the line-emission spectrum that we see when light passes through a prism (usually, many lines of this type). However, if we had a better prism, we would see that real monochromatic sources have a  $I(\sigma)$  that looks more like Figure 6.11(b), where the intensity is nonzero for a small spread of  $\sigma$ s centered about the ideal monochromatic value of  $\sigma_0$ . Information on the  $I(\sigma)$  shown in Figure 6.11(b) is the type of knowledge we get from the Michelson interferometer.

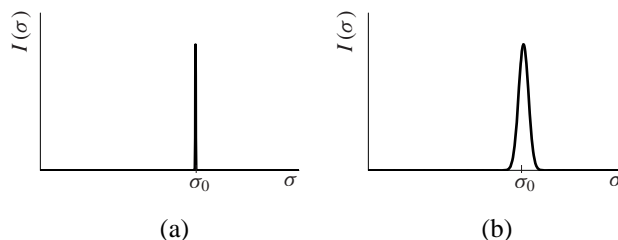


**Figure 6.11**

In the previous paragraph, we called  $I(\sigma)$  an intensity when we talked about the diagrams in Figure 6.11. Actually, it is a more abstract quantity called the spectral intensity designed so that we can use calculus in our description.

### 6.4.2 The spectral intensity $I(\sigma)$

We start with Equation 6.6, which gives the intensity for a single monochromatic source:

$$I(P_0) = \frac{I_0}{8} (1 + \cos \delta) \quad (6.31)$$

where  $P_0$  is at the center of the circular fringe pattern, as illustrated in Figure 6.4. In this section, we want to imagine that we always record the intensity  $I$  at  $P_0$ , where  $\theta = 0$ ,  $\Delta = 2d$ , and  $\delta = (2\pi/\lambda)\Delta = 2\pi\sigma\Delta$  (see Equations 6.11 and 6.12, and remember  $\sigma = 1/\lambda$ ). Thus, we concentrate on how the intensity  $I$  varies with the path difference  $\Delta$ —for this reason, we replace  $P_0$  in Equation 6.31 by  $\Delta$ . To help generalize Equation 6.31 to many sources, we also write it so that we can recognize it as due to source 1:

$$I(\Delta) = I_{01} (1 + \cos 2\pi\sigma_1\Delta) \quad (6.32)$$

where we attach the subscript 1 to  $I_0$  and  $\sigma$  to indicate source 1 (we also include the  $1/8$  in  $I_{01}$  for simplicity). With Equation 6.32 as a guide, we have for two monochromatic sources

$$I(\Delta) = I_{01} (1 + \cos 2\pi\sigma_1\Delta) + I_{02} (1 + \cos 2\pi\sigma_2\Delta) \quad (6.33)$$

and for  $N$  monochromatic sources

$$I(\Delta) = \sum_{n=1}^N I_{0n} (1 + \cos 2\pi\sigma_n\Delta) \quad (6.34)$$

To help us understand the next step to a continuous distribution, we make an analogy with a procedure used in electrostatics for  $N$  point charges on a line, say the  $x$  axis, shown in Figure 6.12(a). The similar diagram for  $N$  monochromatic (or “point”) sources is displayed in Figure 6.12(b). Next, we

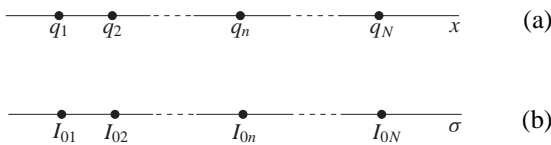


**Figure 6.12** (a) Point charges on the  $x$  axis are analogous to (b) “point-like” sources on the  $\sigma$  axis.

imagine a charge  $Q$  spread continuously along a line, as shown in Figure 6.13(a). To put the problem into the language of calculus, we assume that we know how the charge  $Q$  is spread on the line by knowing  $\lambda(x)$ , the charge density; that is, the charge per unit length in units of say, coulombs/meter. Then, as Figure 6.13(a) indicates, if we take a tiny piece of the line of length  $dx$ , we can say that a point-like charge  $dq$  resides there with  $dq = \lambda(x) dx$ . The total charge  $Q$  on the line would be written as

$$Q = \int_{\text{line}} \lambda(x) dx \quad (6.35)$$

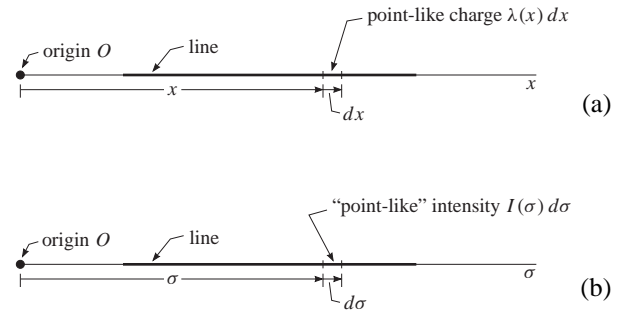


**Figure 6.13** (a) A continuous distribution of charge on a line is analogous to (b) a continuous distribution of light sources on a line.

Likewise, in Figure 6.13(b), we show a continuous distribution of light sources on a line, where  $dI = I(\sigma) d\sigma$  plays the role of a “point-like” source—we put quotes around point-like when referring to a light source, because such a source is usually called a monochromatic one. The special name given to  $I(\sigma)$  is the spectral intensity; however, following the charge analogy, we see it represents an “intensity density” per unit  $\sigma$  with possible units of  $\text{W}/\text{m}^2 \cdot \text{nm}^{-1}$  or  $\text{W}/\text{m}^2 \cdot \text{mm}^{-1}$ . The similar expression to Equation 6.35 is

$$I_0 = \int_{\text{line}} I(\sigma) d\sigma \quad (6.36)$$

Because we take  $I(\sigma)$  to be zero to the left and right of the “heavy” line shown in Figure 6.13(b), we rewrite Equation 6.36 as

$$I_0 = \int_{-\infty}^{\infty} I(\sigma) d\sigma \quad (6.37)$$

which proves to be a more mathematically convenient expression in the work to follow.

Finally, with the concept of the spectral intensity  $I(\sigma)$  and the above analogy, we generalize Equation 6.34 to a continuous distribution:

$$I(\Delta) = \int_{-\infty}^{\infty} I(\sigma) d\sigma (1 + \cos 2\pi\sigma\Delta) = \int_{-\infty}^{\infty} I(\sigma) (1 + \cos 2\pi\sigma\Delta) d\sigma \quad (6.38)$$

### 6.4.3 The visibility $V$

In practice, the intensity  $I(\Delta)$  is the quantity measured with the Michelson interferometer, not the spectral intensity  $I(\sigma)$ . However, to know more about the nature of real sources, it is the spectral intensity  $I(\sigma)$  that we need to determine. One way is to use the concept of Fourier transforms to solve for  $I(\sigma)$  in terms of  $I(\Delta)$ . But it is also instructive to use Michelson’s method, which is the one we use in what follows.

Often  $I(\sigma)$  is centered about some value we shall call  $\sigma_0$ , and it is then convenient to define a new variable  $\sigma'$ , as shown in Figure 6.14. From this diagram, we read

$$\sigma = \sigma_0 + \sigma' \quad (6.39)$$

which gives

$$I(\sigma) = I(\sigma_0 + \sigma') = I(\sigma') \quad (6.40)$$

where normally  $|\sigma'| \ll \sigma_0$  for the range of  $\sigma'$  values that give nonzero values for  $I(\sigma')$ .

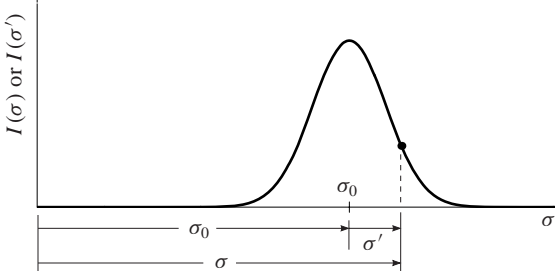


Figure 6.14

Because  $\sigma_0 = \text{constant}$ , when we take differentials of Equation 6.39, we get  $d\sigma = d\sigma'$ . Then, substituting Equations 6.39 and 6.40 into Equation 6.38, we get

$$I(\Delta) = \int_{-\infty}^{\infty} I(\sigma') [1 + \cos 2\pi(\sigma_0 + \sigma')\Delta] d\sigma' \quad (6.41)$$

We use a trig identity to write

$$\begin{aligned} \cos 2\pi(\sigma_0 + \sigma')\Delta &= \cos(2\pi\sigma_0\Delta) \cos(2\pi\sigma'\Delta) \\ &\quad - \sin(2\pi\sigma_0\Delta) \sin(2\pi\sigma'\Delta) \end{aligned} \quad (6.42)$$

which allows us to write Equation 6.41 as

$$\begin{aligned} I(\Delta) &= \int_{-\infty}^{\infty} I(\sigma') d\sigma' \\ &\quad + \cos(2\pi\sigma_0\Delta) \int_{-\infty}^{\infty} I(\sigma') \cos(2\pi\sigma'\Delta) d\sigma' \\ &\quad - \sin(2\pi\sigma_0\Delta) \int_{-\infty}^{\infty} I(\sigma') \sin(2\pi\sigma'\Delta) d\sigma' \\ &= P + (\cos \beta) C(\Delta) - (\sin \beta) S(\Delta) \\ &= P + C(\Delta) \cos \beta - S(\Delta) \sin \beta \end{aligned} \quad (6.43)$$

where

$$\beta = \beta(\Delta) = 2\pi\sigma_0\Delta \quad (6.44)$$

We have written  $\beta(\Delta)$  to indicate that  $\beta$  is really a function of  $\Delta$  just like  $C$  and  $S$  are. We did not indicate this functional

dependence in Equation 6.43 to keep the notation simple. Continuing to inspect Equation 6.43, we see that

$$P = \int_{-\infty}^{\infty} I(\sigma') d\sigma' \quad (6.45a)$$

$$C(\Delta) = \int_{-\infty}^{\infty} I(\sigma') \cos(2\pi\sigma'\Delta) d\sigma' \quad (6.45b)$$

$$S(\Delta) = \int_{-\infty}^{\infty} I(\sigma') \sin(2\pi\sigma'\Delta) d\sigma' \quad (6.45c)$$

We note that  $P$  is a constant. We also note that  $P$  is equal to  $I_0$  in Equation 6.37; however, we use  $P$  to follow practice.

Now we want to get a feeling for the properties of the functions that appear in Equation 6.43. As a first step, we look at the magnitudes of some of the quantities. For He-Ne laser light,  $\lambda = 632.8 \text{ nm}$ , so  $\sigma_0 = 1/\lambda = 1580 \text{ mm}^{-1}$  or  $0.001580 \text{ nm}^{-1}$ . Other wavelengths in the visible produce  $\sigma_0$ s of roughly the same values. We use reciprocal mm as the unit (or sometimes, the reciprocal nm) for the  $\sigma_0, \sigma'$  values for convenience; for then,  $-1 \text{ mm}^{-1} < \sigma' < 1 \text{ mm}^{-1}$  approximately, and  $|\Delta|$  runs from zero to a few mm for many sources. The key is to note how much larger  $\sigma_0$  is compared to  $\sigma'$ . This attribute means that

$$\cos \beta = \cos(2\pi\sigma_0\Delta) \quad \text{and} \quad \sin \beta = \sin(2\pi\sigma_0\Delta)$$

oscillate very rapidly when graphed as a function of  $\Delta$ , but  $C(\Delta)$  and  $S(\Delta)$  in Equations 6.45b and 6.45c change very slowly with  $\Delta$ . So much so that we can treat  $C$  and  $S$  as approximate constants compared to  $\cos \beta$  and  $\sin \beta$  over a reasonable range of  $\Delta$ . To help us understand these properties, we draw an abbreviated graph of  $I(\Delta)$  vs  $\Delta$  for a single spectral line in Figure 6.15 (the graph also extends to the left for negative  $\Delta$ ). We say abbreviated because the graph may extend to the right (and left) a meter or so; we have shortened it to fit in the column. The rapid oscillations are due to  $\sigma_0$ . The  $P$  quantity moves the graph above the  $\Delta$  axis. The  $C$  and  $S$  quantities cause the slow variation (much slower than shown) of the envelope of the curve from large to small.

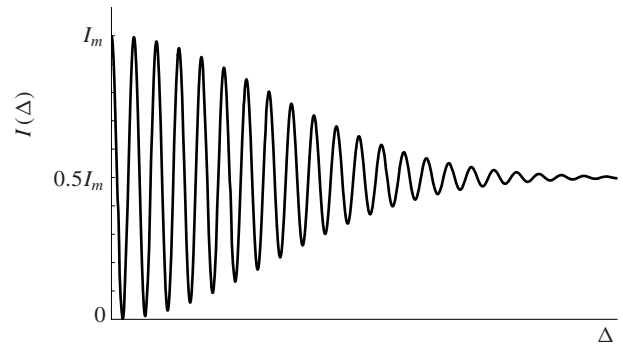


Figure 6.15

To describe the average behavior of  $I(\Delta)$  given in equation form by Equation 6.43, and in approximate picture form by Figure 6.15, we define the visibility  $V$  as

$$V(\Delta) = \frac{I_{\max}(\Delta) - I_{\min}(\Delta+)}{I_{\max}(\Delta) + I_{\min}(\Delta+)} \quad (6.46)$$

To understand the meaning of this equation, we should imagine that we have a graph of  $I(\Delta)$  in front of us. Then,  $I_{\max}(\Delta)$  means that we choose a  $\Delta$  where  $I(\Delta)$  has a maximum and read off the value of  $I(\Delta)$  there. Next, the  $+$  sign in  $I_{\min}(\Delta+)$  says to move to the right of  $\Delta$  to the adjacent minimum, and read off the value of  $I(\Delta)$  at that point. Finally, substitute these values into Equation 6.46, and calculate a value for  $V(\Delta)$ . Continue this process until the entire graph is covered—a great deal of work. However, because the  $I(\Delta)$  has an envelope that varies so slowly, we do not need to choose every maximum and minimum, just representative ones.

To see how this process might work, we redraw Figure 6.15 again as Figure 6.16, and mark off some maximum

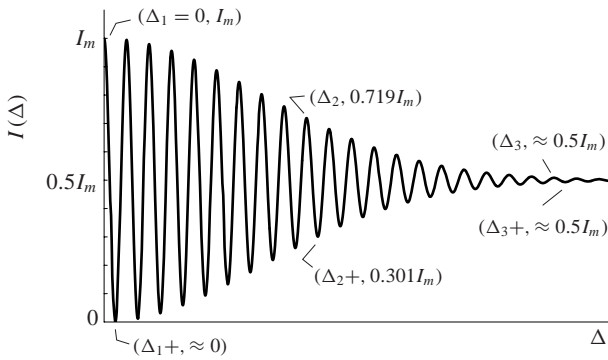


Figure 6.16

and minimum values. We substitute these values into Equation 6.46 and obtain

$$\begin{aligned} V(\Delta_1) &= \frac{I_{\max}(\Delta_1) - I_{\min}(\Delta_1+)}{I_{\max}(\Delta_1) + I_{\min}(\Delta_1+)} \\ &= \frac{I_m - 0}{I_m + 0} = 1 \end{aligned} \quad (6.47a)$$

and similarly

$$V(\Delta_2) = \frac{0.719I_m - 0.301I_m}{0.719I_m + 0.301I_m} = 0.410 \quad (6.47b)$$

$$V(\Delta_3) = \frac{0.5I_m - 0.5I_m}{0.5I_m + 0.5I_m} = 0 \quad (6.47c)$$

By repeating this procedure for a few more points, we would have enough points to draw a graph of  $V$  versus  $\Delta$ , a curve that would vary from a maximum of one to a minimum of zero in this example.

With the help of calculus, we now obtain an expression for  $V(\Delta)$  in terms of the constant  $P$ , and also the slowly varying quantities  $C$  and  $S$ . We start with Equation 6.43, which we rewrite more simply as

$$I(\Delta) = P + C \cos \beta - S \sin \beta \quad (6.48)$$

where (see Equation 6.44)

$$\beta = \beta(\Delta) = 2\pi\sigma_0\Delta \quad (6.49)$$

To find the many maxima and minima of  $I(\Delta)$ , say of the graph in Figure 6.16, we use the standard technique in calculus of taking the derivative of Equation 6.48 and setting it equal to zero. Remembering that we are treating  $C$  and  $S$  as constants, we obtain

$$\begin{aligned} \frac{dI}{d\Delta} &= -C(\sin \beta) \left( \frac{d\beta}{d\Delta} \right) - S(\cos \beta) \left( \frac{d\beta}{d\Delta} \right) = 0 \\ -C(\sin \beta)(2\pi\sigma_0) - S(\cos \beta)(2\pi\sigma_0) &= 0 \\ -C \sin \beta - S \cos \beta &= 0 \\ \frac{\sin \beta}{\cos \beta} &= -\frac{S}{C} \\ \tan \beta &= \frac{-S}{C} = \frac{S}{-C} \end{aligned} \quad (6.50)$$

where we have written the minus sign with first  $S$  and then  $C$  to indicate that there will be two values of  $\beta$  that are solutions to Equation 6.50, one corresponding to maxima, the other corresponding to minima.

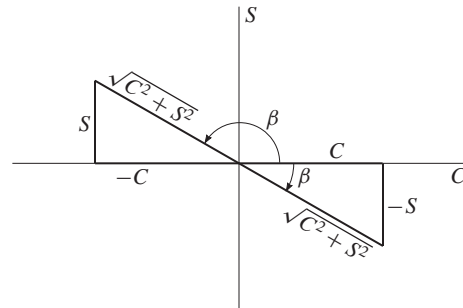


Figure 6.17 Taking  $C$  and  $S$  as positive, Equation 6.50 says that  $\beta$  is in the 4th and 2nd quadrants.

Equation 6.50 helps us draw the diagram in Figure 6.17 from which we read for the cosine function

$$\cos \beta = \frac{C}{\sqrt{C^2 + S^2}} \quad (6.51a)$$

or

$$\cos \beta = \frac{-C}{\sqrt{C^2 + S^2}} \quad (6.51b)$$

In a similar way, we obtain equations for the sine function:

$$\sin \beta = \frac{-S}{\sqrt{C^2 + S^2}} \quad (6.52a)$$

or

$$\sin \beta = \frac{S}{\sqrt{C^2 + S^2}} \quad (6.52b)$$

By inspection of Equations 6.51 and 6.52, we choose the expressions that make  $I(\Delta)$  in Equation 6.48 a maximum or a minimum. We see that the 4th quadrant angle  $\beta$  gives the maxima:

$$\begin{aligned} I_{\max}(\Delta) &= P + C \frac{C}{\sqrt{C^2 + S^2}} - S \frac{-S}{\sqrt{C^2 + S^2}} \\ &= P + \sqrt{C^2 + S^2} \end{aligned} \quad (6.53a)$$

The 2nd quadrant angle  $\beta$  gives the minima:

$$\begin{aligned} I_{\min}(\Delta) &= P + C \frac{-C}{\sqrt{C^2 + S^2}} - S \frac{S}{\sqrt{C^2 + S^2}} \\ &= P - \sqrt{C^2 + S^2} \end{aligned} \quad (6.53b)$$

Recognizing that the  $\Delta+$  we used in Equation 6.46 is not needed here, because Equations 6.53 give expressions for all the maxima and minima, we substitute Equations 6.53 in Equation 6.46 to obtain the visibility:

$$\begin{aligned} V(\Delta) &= \frac{I_{\max}(\Delta) - I_{\min}(\Delta)}{I_{\max}(\Delta) + I_{\min}(\Delta)} \\ &= \frac{(P + \sqrt{C^2 + S^2}) - (P - \sqrt{C^2 + S^2})}{(P + \sqrt{C^2 + S^2}) + (P - \sqrt{C^2 + S^2})} \\ &= \frac{\sqrt{C^2 + S^2}}{P} \end{aligned} \quad (6.54)$$

Michelson guessed at functions for  $I(\sigma')$ , determined the corresponding visibilities  $V$  by calculating  $P$ ,  $C$ , and  $S$ , and then compared the  $V$ s he got with his experimental results. We shall carry out some of these calculations.

#### 6.4.4 Gaussian $I(\sigma')$

Gases when heated to a high temperature produce line spectra when viewed through a prism. If the gas is at low pressure, then it is found that the line broadens due to the Doppler effect; that is, when the atoms/molecules move away from or toward the observer, the wavelength gets longer or shorter, respectively. This broadening is not apparent when the light is viewed through a prism, it still looks like a line. But when viewed with the Michelson interferometer, the broadening effect can be seen.

It is found that an  $I(\sigma')$  curve with the shape called Gaussian gives a visibility  $V$  that agrees with experiment. The functional form for such an  $I(\sigma')$  is

$$I(\sigma') = Ae^{-(\sigma'/a)^2} \quad (6.55)$$

and a graph of this function is shown in Figure 6.18. We characterize the shape of this function by calculating the  $\sigma'$ s that give a value of 1/2 of the maximum  $A$ : we find that  $\sigma' = \pm a\sqrt{\ln 2}$ , as displayed in Figure 6.18; thus

$$\text{HW}_I = \text{half width of } I \text{ at maximum}/2 = a\sqrt{\ln 2} \quad (6.56)$$

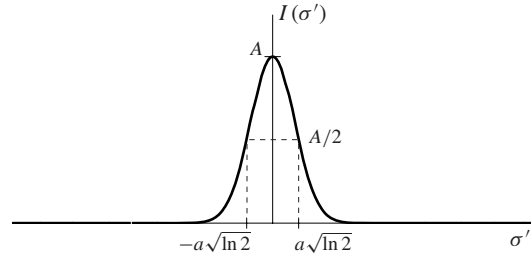


Figure 6.18

To obtain  $V(\Delta)$ , as given by Equation 6.54, we start with Equation 6.45a

$$\begin{aligned} P &= \int_{-\infty}^{\infty} I(\sigma') d\sigma' = \int_{-\infty}^{\infty} Ae^{-(\sigma'/a)^2} d\sigma' \\ &= Aa\sqrt{\pi} \end{aligned} \quad (6.57a)$$

then Equation 6.45b

$$\begin{aligned} C(\Delta) &= \int_{-\infty}^{\infty} I(\sigma') \cos(2\pi\sigma'\Delta) d\sigma' \\ &= \int_{-\infty}^{\infty} Ae^{-(\sigma'/a)^2} \cos(2\pi\sigma'\Delta) d\sigma' \\ &= Aa\sqrt{\pi} e^{-(\pi a\Delta)^2} \end{aligned} \quad (6.57b)$$

and finally Equation 6.45c

$$\begin{aligned} S(\Delta) &= \int_{-\infty}^{\infty} I(\sigma') \sin(2\pi\sigma'\Delta) d\sigma' \\ &= \int_{-\infty}^{\infty} Ae^{-(\sigma'/a)^2} \sin(2\pi\sigma'\Delta) d\sigma' \\ &= 0 \end{aligned} \quad (6.57c)$$

Substituting Equations 6.57 into Equation 6.54, we get

$$V(\Delta) = \frac{\sqrt{C^2 + S^2}}{P} = e^{-(\pi a\Delta)^2} \quad (6.58)$$

A graph of  $V(\Delta)$  is displayed in Figure 6.19. The  $\Delta$  values that give 1/2 of the maximum 1 are found to be  $\pm\sqrt{\ln 2}/\pi a$ , and are indicated on the graph; thus,

$$\text{HW}_V = \text{half width of } V \text{ at } 1/2 \text{ maximum} = \frac{\sqrt{\ln 2}}{\pi a} \quad (6.59)$$

We note that the half widths of the graphs of  $I(\sigma')$  and  $V(\Delta)$  are inversely related to each other; that is, a narrow  $I(\sigma')$  means a wide  $V(\Delta)$ . If we multiply these two half widths together, we get a constant:

$$\text{HW}_I \text{HW}_V = \left(a\sqrt{\ln 2}\right) \left(\frac{\sqrt{\ln 2}}{\pi a}\right) = \frac{\ln 2}{\pi} \quad (6.60)$$

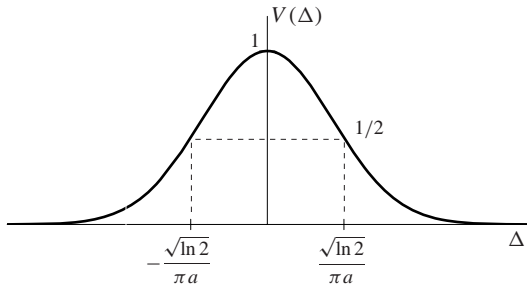


Figure 6.19

### 6.4.5 Lorentzian $I(\sigma')$

Gases at high temperature and high pressure have a different  $I(\sigma')$  because, in addition to the Doppler effect discussed in the previous section, collisions between the atoms or molecules becomes important. In this case,

$$I(\sigma') = \frac{A}{\sigma'^2 + a^2} \quad (6.61)$$

called a Lorentzian function. A graph of this function is shown in Figure 6.20. From Equation 6.61 we calculate the  $\sigma'$  values that give 1/2 the maximum of  $A^2/a^2$  to be  $\pm a$ ; we indicate these values in Figure 6.20, and we have

$$\text{HW}_I = \text{half width of } I \text{ at } 1/2 \text{ maximum} = a \quad (6.62)$$

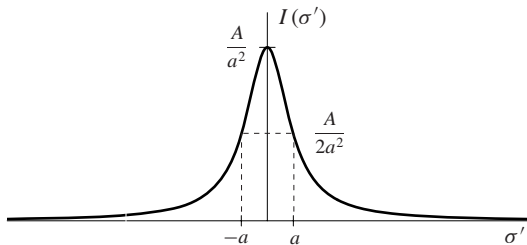


Figure 6.20

As we performed in the previous section, we use Equations 6.45 to calculate

$$\begin{aligned} P &= \int_{-\infty}^{\infty} I(\sigma') d\sigma' = \int_{-\infty}^{\infty} \frac{A}{\sigma'^2 + a^2} d\sigma' \\ &= \frac{\pi A}{a} \end{aligned} \quad (6.63a)$$

$$\begin{aligned} C(\Delta) &= \int_{-\infty}^{\infty} I(\sigma') \cos(2\pi\sigma'\Delta) d\sigma' \\ &= \int_{-\infty}^{\infty} \frac{A}{\sigma'^2 + a^2} \cos(2\pi\sigma'\Delta) d\sigma' \\ &= \frac{\pi A}{a} e^{-2\pi a|\Delta|} \end{aligned} \quad (6.63b)$$

$$\begin{aligned} S(\Delta) &= \int_{-\infty}^{\infty} I(\sigma') \sin(2\pi\sigma'\Delta) d\sigma' \\ &= \int_{-\infty}^{\infty} \frac{A}{\sigma'^2 + a^2} \sin(2\pi\sigma'\Delta) d\sigma' \\ &= 0 \end{aligned} \quad (6.63c)$$

Substituting these equations into Equation 6.54, we obtain the visibility  $V$  corresponding to a Lorentzian spectral line:

$$V(\Delta) = \frac{\sqrt{C^2 + S^2}}{P} = \frac{\pi A}{a} e^{-2\pi a|\Delta|} \quad (6.64)$$

A graph of Equation 6.64 is shown in Figure 6.21, and we calculate

$$\begin{aligned} \text{HW}_V &= \text{half width of } V \text{ at } 1/2 \text{ maximum} \\ &= \frac{\ln 2}{2\pi a} \end{aligned} \quad (6.65)$$

Then

$$\text{HW}_I \text{HW}_V = (a) \left(\frac{\ln 2}{2\pi a}\right) = \frac{\ln 2}{2\pi} \quad (6.66)$$

a constant, just as in Equation 6.60.

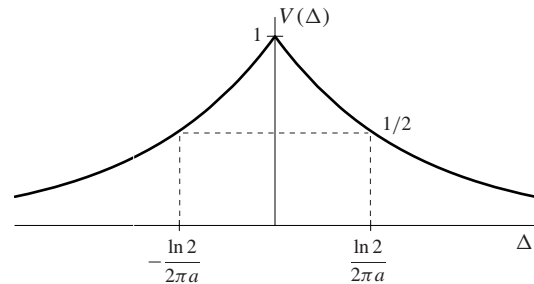


Figure 6.21

### 6.4.6 Sodium-like D lines $I(\sigma')$

When sodium is heated to a high temperature, it emits a noted emission spectrum of two bright, yellow lines that are very close together. One wavelength is  $\lambda_1 = 588.995$  nm, the slightly longer wavelength is  $\lambda_2 = 589.592$  nm, for a separation of  $\Delta\lambda = 0.597$  nm. The spectral intensity  $I(\sigma')$  is made of two separated Gaussian curves (see Equation 6.55) with the longer wavelength curve having a maximum that is 80%, or 4/5, that of the shorter wavelength maximum. We write the spectral intensity for a sodium-like substance as

$$I(\sigma') = A e^{-(\sigma'+b)^2/a^2} + (4/5)A e^{-(\sigma'-b)^2/a^2} \quad (6.67)$$

which has the graph shown in Figure 6.22.

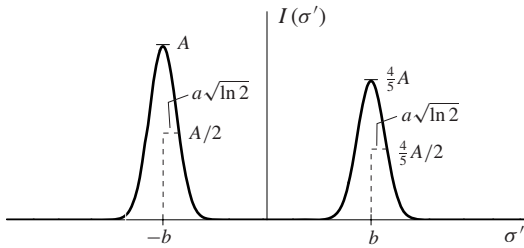


Figure 6.22

Substituting Equation 6.67 into Equations 6.45, we obtain expressions for  $P$ ,  $C$ , and  $S$ :

$$\begin{aligned} P &= \int_{-\infty}^{\infty} I(\sigma') d\sigma' \\ &= \int_{-\infty}^{\infty} \left[ A e^{-(\sigma'+b)^2/a^2} + (4/5)A e^{-(\sigma'-b)^2/a^2} \right] d\sigma' \\ &= \frac{9}{5}\sqrt{\pi}Aa \end{aligned} \quad (6.68a)$$

$$\begin{aligned} C(\Delta) &= \int_{-\infty}^{\infty} I(\sigma') \cos(2\pi\sigma'\Delta) d\sigma' \\ &= \int_{-\infty}^{\infty} \left[ A e^{-(\sigma'+b)^2/a^2} + (4/5)A e^{-(\sigma'-b)^2/a^2} \right] \cos(2\pi\sigma'\Delta) d\sigma' \\ &= \frac{9}{5}\sqrt{\pi}Aae^{-(\pi a\Delta)^2} \cos(2\pi b\Delta) \end{aligned} \quad (6.68b)$$

$$\begin{aligned} S(\Delta) &= \int_{-\infty}^{\infty} I(\sigma') \sin(2\pi\sigma'\Delta) d\sigma' \\ &= \int_{-\infty}^{\infty} \left[ A e^{-(\sigma'+b)^2/a^2} + (4/5)A e^{-(\sigma'-b)^2/a^2} \right] \sin(2\pi\sigma'\Delta) d\sigma' \\ &= -\frac{1}{5}\sqrt{\pi}Aae^{-(\pi a\Delta)^2} \sin(2\pi b\Delta) \end{aligned} \quad (6.68c)$$

Finally, as we have done before, we substitute Equations 6.68 into Equation 6.54, and after simplification, we obtain the visibility  $V$  for sodium-like spectra:

$$\begin{aligned} V(\Delta) &= \frac{\sqrt{C^2 + S^2}}{P} \\ &= \frac{1}{9} e^{-(\pi a\Delta)^2} \sqrt{41 + 40 \cos(4\pi b\Delta)} \end{aligned} \quad (6.69)$$

The graph of this equation is shown in Figure 6.23.

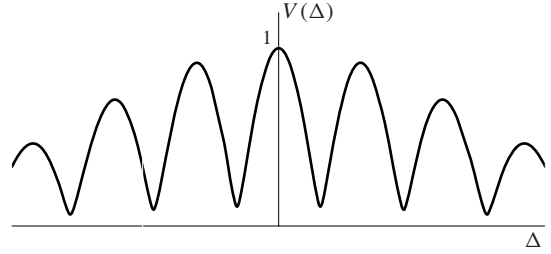


Figure 6.23

Suppose we wish to determine the  $\Delta$  positions of the maxima and minima of the curve in Figure 6.23. Inspecting Equation 6.69, we would expect the maxima and minima are given approximately by setting  $\cos(4\pi b\Delta)$  equal to  $+1$  or  $-1$ , respectively. We say approximately, because the exponential in front of the square root has a small effect, and we would expect the effect to be smaller for the minima because smaller numbers are involved. So, we look at the minima; for convenience, just those for positive  $\Delta$ —these minima occur when  $\cos(4\pi b\Delta)$  equals  $-1$ ; that is, when  $4\pi b\Delta$  equals odd multiples of  $\pi$ , or

$$\begin{aligned} 4\pi b\Delta &= (2m+1)\pi \\ \Delta_m &= \frac{2m+1}{4b}, \quad m = 0, 1, 2, \dots \end{aligned} \quad (6.70)$$

where we attach the subscript  $m$  to  $\Delta$  to make a useful notation. The separation  $s$  between adjacent minima is a constant, as we see from application of Equation 6.70:

$$\begin{aligned} s = \Delta_{m+1} - \Delta_m &= \frac{2(m+1)+1}{4b} - \frac{2m+1}{4b} \\ &= \frac{1}{2b} \end{aligned} \quad (6.71)$$

Equation 6.71 implies that if we experimentally obtain a graph of  $V(\Delta)$ , then we can measure  $s$  from the graph, and calculate

$$2b = \frac{1}{s} \quad (6.72)$$

which equals the separation of the lines in Figure 6.22.

## PROBLEMS

- 6.1** Suppose  $d = 5150$  nm and  $\lambda = 546.1$  nm. (a) Calculate  $d$  and  $\lambda$  in m and mm. (b) Use Equation 6.3 to calculate the phase difference  $\delta$  in rad and deg.
- 6.2** Suppose  $\delta$  has the value in Problem 6.1. (a) In what quadrant is  $\delta$ ? (b) Use Equation 6.9 to calculate  $I/I_m$ .
- 6.3** Suppose  $d = 5150$  nm,  $\lambda = 546.1$  nm, and  $\theta = 0.1$  rad. Calculate (a)  $\Delta$ , (b)  $\delta$ , and (c)  $I/I_m$ .
- 6.4** If  $\theta = 0.100$  rad and  $f' = 100$  mm, calculate  $r$ .
- 6.5** Calculate the values of the order number  $m$  for bright fringes of a monochromatic source when  $d/\lambda$  has the values of (a) 1, (b) 3, (c) 4.9, and (d) 100, respectively. The ratio  $r/f'$  satisfies the inequality relation  $0 \leq r/f' \leq 1$ .
- 6.6** Suppose that  $d/\lambda = 7.6$  and that  $r/f'$  ranges from zero to unity. Determine the order numbers for the bright fringes that are seen in the field of view?
- 6.7** Given that  $d = 5150$  nm,  $\lambda_1 = 590$  nm,  $\lambda_2 = 591$  nm, and  $\theta = 0.15$  rad. Calculate (a)  $\Delta$ , (b)  $\delta_1$ , and (c)  $\delta_2$ . Then determine (d)  $I_1/I_m$ , (e)  $I_2/I_m$ , and (f)  $I_{\text{tot}}/I_m$ .
- 6.8** (a) Show all the steps to derive Equation 6.24a. (b) Do the same for deriving Equation 6.24b.
- 6.9** Note that in the graphs of Figure 6.9 that  $r/f'$  has a maximum value of 1/10 in the discussion of a doublet. Obtain two equations similar to Equation 6.24a for a doublet: (a) one equation should be for  $m_1$  and  $\lambda_1$ , (b) the other for  $m_2$  and  $\lambda_2$ .
- 6.10** If we require that  $r/f' \leq h$  and  $d \geq 0$ , then get a more general form for the left side of the inequality in Equation 6.24a.
- 6.11** Use the two inequality equations you derived in Problem 6.9 and substitute the  $\lambda$  values for sodium given in Equation 6.26. Then obtain the allowed  $m_1$  and  $m_2$  values for the  $d$  values used in Figures 6.9; namely, for the values of (a)  $d = 146,000$  nm, (b)  $d = 200,000$  nm, and (c)  $d = 300,000$  nm.
- 6.12** The visible spectrum runs from about  $\lambda_1 = 400$  nm to  $\lambda_2 = 700$  nm. Calculate the corresponding wave numbers  $\sigma_1$  to  $\sigma_2$  in  $\text{nm}^{-1}$  and  $\text{mm}^{-1}$ .
- 6.13** Remembering that for an even function  $f(-x) = f(x)$  and for an odd function  $f(-x) = -f(x)$ , show that the following functions are even, odd, or neither: (a)  $\sin bx$ , (b)  $\cos bx$ , (c)  $e^{-x}$ , (d)  $e^{-x^2}$ , (e)  $\sin bx^2$ , and (f)  $\sin bx^3$ . Assume that the coefficient  $b$  is a constant.
- 6.14** Given that
- $$I(\sigma') = 10e^{-(\sigma'/5)^2}$$
- (a) If  $\sigma'$  is measured in  $\text{mm}^{-1}$ , what units would 5 have? (b) Determine  $\text{HW}_I$ .
- 6.15** Suppose
- $$V(\Delta) = e^{-15\Delta^2}$$
- with  $\Delta$  measured in mm. (a) What is  $a$  equal to? (b) Determine  $\text{HW}_V$ . (c) Write the corresponding  $I(\sigma')$  if  $A = 5 \text{ W/m}^2 \cdot \text{mm}^{-1}$ .
- 6.16** Show the algebra for obtaining the  $\sigma'$  values that make  $I(\sigma')$  equal to  $A/2$  in Equation 6.55; that is, half the maximum value of  $A$ .
- 6.17** (a) Find the maximum of  $I(\sigma')$  in Equation 6.61. (b) Determine the  $\sigma'$  values that make this  $I(\sigma')$  equal to half its maximum.
- 6.18** Guess at some values for  $a$  and  $b$  to substitute into Equation 6.69, then write a computer program to get a graph that looks somewhat like the one shown in Figure 6.23.



**Page intentionally left blank.**

## Chapter 6: Answers to Problems

- 6.1** (a)  $5.15 \times 10^{-6}$  m,  $5.15 \times 10^{-3}$  mm;  
 $5.461 \times 10^{-7}$  m,  $5.461 \times 10^{-4}$  mm;  
 (b) 118.5 rad, 6790 deg

**6.2** (a) 4th; (b) 0.821

**6.3** (a) 0.01025 mm; (b) 117.9 rad; (c) 0.553

**6.4** 10.0 mm

**6.5** (a) 2; (b) 5, 6; (c) 7, 8, 9; (d) 142, 143, . . . , 200

**6.6** 11, 12, 13, 14, 15

**6.7** (a) 10184.3 nm; (b) 108.458 rad; (c) 108.274 rad;  
 (d) 0.232; (e) 0.278; (f) 0.509

- 6.9** (a)  $\frac{20}{\sqrt{101}} \frac{d}{\lambda_1} \leq m_1 \leq 2 \frac{d}{\lambda_1}$   
 (b)  $\frac{20}{\sqrt{101}} \frac{d}{\lambda_2} \leq m_2 \leq 2 \frac{d}{\lambda_2}$

$$\mathbf{6.10} \quad \frac{2}{\sqrt{h^2 + 1}} \frac{d}{\lambda} \leq m$$

- 6.11** (a)  $m_1 = 494, 495$ ;  $m_2 = 493, 494, 495$ ;  
 (b)  $m_1 = 676, 677, 678, 679$ ;  $m_2 = 676, 677, 678$ ;  
 (c)  $m_1 = 1014, 1015, 1016, 1017, 1018$ ;  
 $m_2 = 1013, 1014, 1015, 1016, 1017$

**6.12**  $0.0025 \text{ nm}^{-1}$ ,  $0.001429 \text{ nm}^{-1}$ ;  
 $2500 \text{ mm}^{-1}$ ,  $1429 \text{ mm}^{-1}$

**6.13** (a) odd; (b) even; (c) neither; (d) even; (e) even; (f) odd

**6.14** (a)  $\text{mm}^{-1}$ ; (b)  $4.16 \text{ mm}^{-1}$

**6.15** (a)  $\frac{\sqrt{15}}{\pi} \text{ mm}^{-1}$ ; (b)  $5e^{-(\pi\sigma'/\sqrt{15})^2}$

**6.16**  $\pm a\sqrt{\ln 2}$

**6.17** (a)  $A/a^2$ ; (b)  $\pm a$